



Original article

DNA fastening and ripping actions of novel Knoevenagel condensed dicarboxylic acid complexes in antitumor journey



Natarajan Raman*, Narayanaperumal Pravin

Research Department of Chemistry, VHNSN College, Virudhunagar 626 001, Tamil Nadu, India

ARTICLE INFO

Article history:

Received 18 November 2013

Received in revised form

18 March 2014

Accepted 8 April 2014

Available online 13 April 2014

Keywords:

Oxali-platin type complexes

Intercalative mode

DNA cleavage

Cytotoxicity

Antitumor effect

ABSTRACT

Few novel Cu(II) and Zn(II) oxali-platin type complexes of stoichiometry $[ML(ox)]$ where, L is a Knoevenagel ligand and ox is oxalic acid, have been explored. They are well characterized by spectroanalytical methods. The binding and cleavage propensity of these complexes on DNA and their cytotoxic effect in tumor cells have been investigated. They bind to DNA preferentially by intercalation and cleave the strands under mild reaction conditions even in the absence of external cofactors. However, in H_2O_2 medium they exhibit better efficacy in the nuclease reaction process by initiating DNA cleavage in an oxidative pattern. Complex **1** shows higher *in vitro* cytotoxic property against HeLa/EAC cells comparing to other complexes and the standards (cisplatin/5-FU). Moreover, the *in vivo* antitumor efficacy of copper complexes against EAC tumor model reveals that they are non-toxic to normal cells (lymphocytes). Among the copper complexes, complex **1** reveals excellent antitumor activity.

© 2014 Elsevier Masson SAS. All rights reserved.

1. Introduction

The major focus of research in chemotherapy for cancer in recent times includes the identification, characterization and development of new and safe cancer chemopreventive agents [1]. Over the past 30 years platinum compounds have played a very important and well documented role in treating cancer [2,3]. Especially, oxali-platin, as the prototype of the third-generation platinum drugs which are characterized by substitution of both the amine carrier ligands and the labile chlorido leaving groups of cisplatin with 1,2-diaminocyclohexane (1,2-DACH) and carboxylato groups, possesses rare cross-resistance with cisplatin, appropriate water-solubility and reduced toxicity. Also, it is the first platinum-based chemotherapeutics in the treatment of metastatic colorectal cancer [4]. As it possesses inherent limitations such as lesser side effects, general toxicity, and acquired drug resistance, attempts are being made to replace the platinum-based drugs with suitable alternatives, and numerous metal based complexes are synthesized and screened for their anticancer activities. Further, the non-platinum antitumor compounds show various geometries and coordination numbers, various oxidation states, better solubility, feasible substitution kinetic pathways and factors influencing the

pharmacological profile different than those of platinum drugs [5,6]. Many authentic reports are available in the literature which reveals the anticancer activity of the non-platinum transition metal complexes containing oxygen and nitrogen donors [7]. Large number of studies has been carried out on non-platinum transition metal complexes for their ability to mediate oxidative damage to nucleobases and/or to the 2-deoxyribose moiety in presence of oxidizing or reducing agent, light, or redox-active metal center [8–11].

Recently, few of the mono-, di- and multinuclear metal complexes of Cu(II), Fe(III), Zn(II), Ru(II), Co(III), Ln(III)/(IV) with azamacrocyclic, aminocarboxylic, pyridyl, benzimidazolyl, ferrocenyl and others are reported to show strong chemical nucleases activity under physiological conditions [12]. Compared with other transition metals, Cu(II) ion has relatively strong Lewis acidity and high nucleobase affinity to induce efficient DNA cleavage activity. Generally, copper is a biometal and its complexes are less toxic and some of them have even important cellular effects such as neurotransmission, cellular respiration and others. Recent studies on new kinds of chemotherapeutic Schiff bases are now attracting the attention of biochemists. The coordination behavior of β -diketone derivatives also has significant influences on the relative stabilities of the mixed-ligand complexes as well as their use in biomedicine [13,14]. Moreover, the emerging Knoevenagel condensate Schiff base metal complexes have been a wide variety of applications in various fields, like agriculture, industry, pharmaceutical etc., [15,16]. In this regard, N_2O_2 mixed-ligand metal complexes are

* Corresponding author.

E-mail addresses: ramchem1964@gmail.com, drn_raman@yahoo.co.in (N. Raman), pravinknp2012@gmail.com (N. Pravin).

found to be particularly useful because of their potential to bind DNA via a multitude of interactions and to cleave the duplex by virtue of their intrinsic chemical, electrochemical, and photochemical activities [17,18].

Over the last few years, dicarboxylic acids [19–21] and the oxalate containing compounds hold an active field of research in the systematic construction of mixed ligand metal complexes with interesting properties in biological systems towards applications in biological chemistry, catalysis, photochemistry and magnetochemistry [22]. Also, this is widely used in crystal engineering that may serve as “templates” for new functional materials [23,24].

Based on the above facts, we are tempted to develop new non-platinum anticancer agents. In continuation of our journey in designing and exploring the newer anticancer agents [25] in order to improve the anticancer efficacy, we hereby report the synthesis and characterization of few new oxali-platin type copper(II) and zinc(II) complexes. Herein, the *in vitro* and *in vivo* antitumor activities against two human cancer cell lines (HeLa and MCF-7) and animal tumor cell line (EAC) have been evaluated.

2. Chemistry

The novel Knoevenagel condensate Schiff bases L^1 – L^4 and their mixed-ligand (i.e., oxalic acid) Cu(II) and Zn(II) complexes were synthesized and characterized by spectral and elemental analysis data. The complexes were found to be air stable. The ligands are soluble in common organic solvents but their complexes are soluble only in DMF and DMSO. The results of elemental analysis for the metal complexes are in good agreement with the calculated values showing that the complexes have 1:1:1 (Knoevenagel condensate Schiff base: metal: oxalic acid) stoichiometry of the type [ML(ox)] wherein L acts as a bidentate ligand. The metal(II) complexes were dissolved in DMF and the molar conductivities of 10^{-3} M of their solution at room temperature were measured. The lower conductance values (8.3 – $15.2 \Omega^{-1} \text{ cm}^{-2} \text{ mol}^{-1}$) of the complexes support their non-electrolytic nature.

3. Pharmacology

The DNA binding study of the synthesized complexes with CT DNA was carried out by electronic absorption spectroscopy, viscosity measurements and cyclic voltammetry techniques. The extent of pBR322 DNA cleavage, in the absence and presence of an activating agent H_2O_2 and various radical scavengers like sodium azide (singlet oxygen), SOD (superoxide), DMSO (hydroxyl radical scavenger), was monitored using agarose gel electrophoresis. A meticulous sympathetic of the structural and electronic properties of drug-DNA complexes and their mechanism of binding is the key step in elucidating the principles of their anti-cancer activity. *In vitro* and *in vivo* anti-tumor functions of synthesized complexes against Ehrlich ascites carcinoma (EAC) tumor model were investigated. The antitumor activity was assessed by hematological parameters, median survival time and cell viability with trypan blue dye exclusion assay. *In vitro* cytotoxicity was performed by MTT assay against human cervical cancer cell lines (HeLa) and Human breast cancer lines (MCF-7). The minimum inhibitory concentration (MIC) values of the complexes were determined.

4. Results and discussion

The formation of the investigated Schiff bases and their mixed ligand complexes is represented in Scheme 1. The ligands and their complexes are found to be stable in air. The ligands are soluble in common organic solvents but their complexes are soluble only in DMF and DMSO.

4.1. Infrared spectra

The tentative assignments of the IR bands are useful tools for determining the coordination mode of the ligands with metal ions. There are some elevated peaks in the spectra of the ligands which are good in accomplishing this goal. The position and/or the intensities of these peaks are expected to be changed upon chelation. The bands observed in the range of 1638 – 1631 cm^{-1} for the azomethine group $\nu(\text{C}=\text{N})$ authenticating an effective Schiff base condensation between 3-benzylidene-pentane-2,4-dione and *p*-substituted anilines, have undergone a negative shift in the complexes in the range of 1615 – 1601 cm^{-1} ca. 30 cm^{-1} on comparing with the free ligands. This may be explained on the basis of a drift of lone pair density of azomethine nitrogen towards the metal ions suggesting that the coordination takes place through nitrogen of $\nu(\text{C}=\text{N})$ [26]. Besides, the free $-\text{OH}$ group of the ligand L^3 vibrated at ca. 3430 cm^{-1} does not show any significant shift on complex formation, which confirms that the phenolic group is not participated on complex formation.

The additional bands in complexes at 1686 , 1347 and 816 cm^{-1} could be ascribed to the vibrations of the oxalic acid moiety. This suggests the presence of dicarboxylic acid as a bidentate ligand in the metal(II) centers via two monodentate carboxylate groups. The mixed oxalato complexes show the stretching vibration of $\nu\text{C}=\text{O}$ of the oxalate groups at 1689 – 1681 cm^{-1} . The relatively high value for this group indicates the unsharing of the $\text{C}=\text{O}$ group in coordination to metal ion and thus the oxalato group acts as a dianionic bidentate ligand. This is further confirmed by the formation of metal–oxygen bond in the complexes in the region 505 – 533 cm^{-1} . The new band observed in the complexes in the range 448 – 430 cm^{-1} indicates the formation of $\text{M}-\text{N}$ bond.

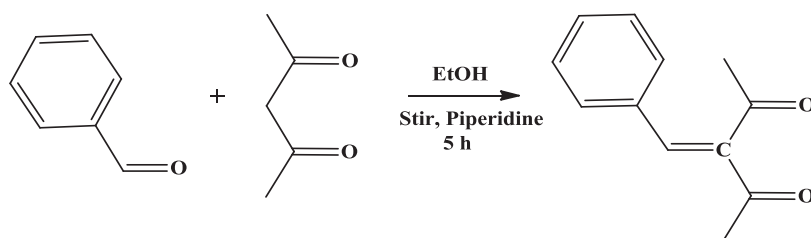
4.2. Elemental analysis and molar conductivity measurements

The results of elemental analysis for the metal complexes are in good agreement with the calculated values showing that the complexes have 1:1:1 metal–ligand stoichiometry of the type [ML(ox)] wherein L and (ox) act as bidentate ligands (Scheme 1). The complexes are found to be non-electrolytic nature in 10^{-3} M DMF solution, implying the replace of chloride anions by bidentate oxalate to the central metal ion. The absence of counter (chloride) ion is conformed from Volhard's test. The molar conductance values (8.3 – $15.2 \Omega^{-1} \text{ cm}^{-2} \text{ mol}^{-1}$) of the complexes support their non-electrolytic nature.

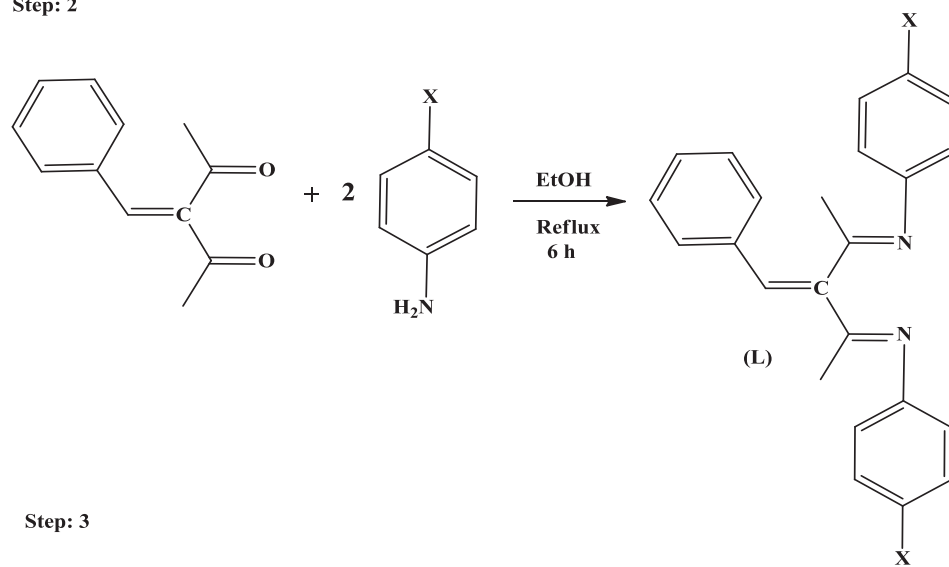
4.3. Magnetic moments and electronic spectra

The electronic absorption spectra are often very helpful in the evaluation of results furnished by other methods of structural investigation. The geometry of the metal complexes has been deduced from electronic spectra and magnetic data of the complexes, which were recorded in DMF solution. The free ligands exhibit two intense bands in $45,857$ – $41,656$ and $28,361$ – $27,138 \text{ cm}^{-1}$ region due to $\pi \rightarrow \pi^*$ and $n \rightarrow \pi^*$ transitions [27], respectively. In all the metal complexes, the absorption bands at $40,475$ – $43,836$ and $29,561$ – $35,225 \text{ cm}^{-1}$ are due to $\pi \rightarrow \pi^*$ and $n \rightarrow \pi^*$ transitions that are observed in the spectra of the free ligands L^1 , L^2 , L^3 and L^4 . These transitions are shifted to blue or red frequencies due to the coordination of the ligand with metal ions. The electronic spectra of Cu(II) complexes (1–4) show broad bands at around $22,883$ – $23,364 \text{ cm}^{-1}$, which are assigned to the ${}^2\text{B}_{1g} \rightarrow {}^2\text{A}_{1g}$ transition which is characteristic of distorted square planar environment around the copper(II) ion. The observed

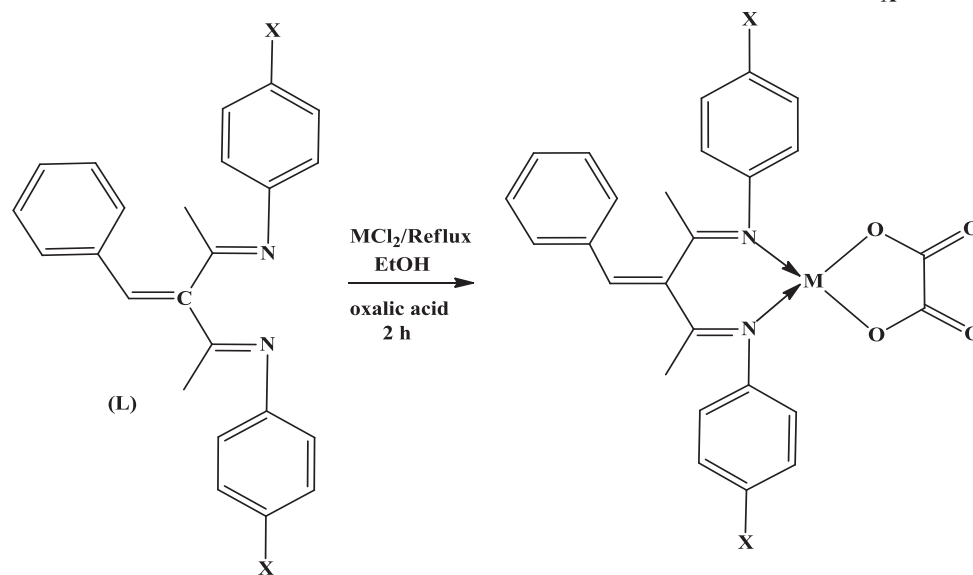
Step: 1



Step: 2



Step: 3



M	X	Complex
Cu(II)/Zn(II)	-NO ₂ (L ¹)	CuL ¹ (ox) (1)/ZnL ¹ (ox) (5)
Cu(II)/Zn(II)	-H (L ²)	CuL ² (ox) (2)/ZnL ² (ox) (6)
Cu(II)/Zn(II)	-OH (L ³)	CuL ³ (ox) (3)/ZnL ³ (ox) (8)
Cu(II)/Zn(II)	-OCH ₃ (L ⁴)	CuL ⁴ (ox) (4)/ZnL ⁴ (ox) (9)

Scheme 1. Synthesis of Schiff base ligands and their metal complexes.

magnetic moment of the Cu(II) complexes (**1–4**) (1.84–1.88 B.M) at room temperature indicates the non-coupled mononuclear complexes of magnetically diluted d⁹ system with S = 1/2 spin-state. The monomeric nature of the complexes is further supported by

the microanalytical and ESI mass spectral data. The electronic absorption spectra of the diamagnetic Zn(II) complexes show the bands at 40,561–42,359 and 29,198–33,853 cm⁻¹ which are assigned to intra-ligand charge transfer transitions [28].

4.4. NMR spectra of Zn(II) complexes

In ^1H NMR, the aromatic region is a set of multiplets in the range of 6.8–7.4 ppm for all the ligands and their Zn(II) complexes. The phenolic –OH proton for L^3 ligand and its Zn(II) complex is observed as a singlet at ca. 10.3 ppm. It is suggesting that phenolic –OH group is not taking part in the complexation. ^1H NMR spectra of aliphatic methyl protons exhibit at 2.1–2.4 ppm for all the Schiff base ligands and their Zn(II) complexes. There is no appreciable change in all other signals of the complexes. The spectra of ligand L^4 and its complex **8** are given in Figs. S1a and S1b (Supplementary file).

The ^{13}C NMR spectra of the ligands show aromatic carbons at 119–129 ppm. The ligands also show the C=N carbons at 172.8–175.4 ppm, which are shifted to downfield at 168.2–170.4 ppm, upon coordination indicating that the C=N groups participate in complex formation. The peak at 164.3–168.7 ppm of Zn(II) complexes indicates the presence of oxalic acid carbon moiety. The ^{13}C NMR spectra of ligand L^4 and its complex **8** are given in Figs. S2a and S2b. Comparison of all carbon peaks of the ligands with those of Zn(II) complexes show some upfield and downfield shifts, but these shifts are not so large. This indicates the coordination of the ligand to the metal ion.

4.5. Mass spectra

The ESI-mass spectra of synthesized ligands and their complexes were recorded and the obtained molecular ion peaks confirm the proposed formulas. The mass spectrum of L^1 ligand shows $[\text{M} + 1]$ peak at m/z 429 (86.4%) corresponding to $[\text{C}_{24}\text{H}_{20}\text{N}_4\text{O}_4]^+$ ion. Also, the spectrum exhibits the fragments at m/z 184, 102 and 77 corresponding to $[\text{C}_{12}\text{H}_{12}\text{N}_2]^+$, $[\text{C}_8\text{H}_5]^+$ and $[\text{C}_5\text{H}_6]^+$ respectively. The mass spectrum of complex **1** shows peaks at m/z 581 with 65.2% abundances, respectively. The strongest peaks (base peak) at m/z 429 represent the stable species $\text{C}_{24}\text{H}_{20}\text{N}_4\text{O}_4$. Moreover, the spectrum exhibits the fragments at m/z 184, 102 and 77 corresponding to $[\text{C}_{12}\text{H}_{12}\text{N}_2]^+$, $[\text{C}_8\text{H}_5]^+$ and $[\text{C}_5\text{H}_6]^+$ respectively. The m/z of all the fragments of ligands and their complexes confirm the stoichiometry of the complexes as $[\text{ML}^1(\text{ox})]$. The observed peaks are in good agreement with their formulas as expressed from microanalytical data. Thus, the mass spectral data reinforce the conclusion drawn from the analytical and conductance values.

4.6. EPR spectra

The EPR spectra of Cu(II) complexes (**1–4**) provide information about hyperfine and super hyperfine structures. It is very important to understand the metal ion environment in the complexes, i.e., the geometry, nature of the donating atoms from the ligands and degree of covalency of the Cu(II)–ligand bonds. The X-band EPR spectra of all Cu(II) complexes (**1–4**) have been recorded in DMSO at liquid nitrogen temperature and at room temperature. The spectra of the Cu(II) complexes at RT show one intense absorption band in the high field and are isotropic due to the tumbling motion of the molecules. However, these complexes at LNT show three-well resolved peaks with low field region. The spin Hamiltonian parameters of the complexes were calculated and are summarized in Table 1. From this spectral data, it is found that A_{\parallel} (142–151) > A_{\perp} (23–27); g_{\parallel} (2.22–2.15) > g_{\perp} (2.05–2.03) > g_e (2.0023), which support the $d_{x^2-y^2}$ as the ground state, characteristic of square-planar geometry and axially symmetric. Further, in an axial symmetry, the G -values are related by the expression,

Table 1

The spin Hamiltonian parameters of the Cu(II) complexes in DMSO solution at 77 K.

Complexes	g-tensor			$A \times 10^{-4} (\text{cm}^{-1})$			$g_{\parallel}/A_{\parallel}$	G
	g_{\parallel}	g_{\perp}	g_{iso}	A_{\parallel}	A_{\perp}	A_{iso}		
1	2.15	2.04	2.08	149	25	66	144	4.12
2	2.19	2.03	2.09	145	23	64	151	5.02
3	2.22	2.05	2.11	142	27	65	156	4.41
4	2.21	2.04	2.10	151	24	66	146	5.63

$$G = (g_{\parallel} - 2) / (g_{\perp} - 2)$$

which measures the exchange interaction between the copper centers in polycrystalline solid. The G values lie within the range 4.12–5.63 for all the Cu(II) complexes indicating negligible exchange interaction of Cu–Cu in the complexes according to Hathaway [29]. The empirical factor $f = g_{\parallel}/A_{\parallel} \text{ cm}^{-1}$ is an index of tetragonal distortion. Values of this factor may vary from 105 to 135 for small to extreme distortions in square planar complexes and it depends on the nature of the coordinated atoms. The f values of copper complexes (**1–4**) are in the range from 144–156, indicating significant distortion from planarity. The EPR studies of the Cu(II) complexes have provided supportive evidence to the conclusion obtained on the basis of electronic and magnetic moment values.

4.7. DNA binding studies

4.7.1. Absorption titration measurement

Most of the antitumor drugs act by targeting DNA and therefore, DNA binding is one of the most critical steps for the action of a large number of metal based anticancer drugs. Electronic absorption spectroscopy is used as a distinctive characterization tool for examining the binding mode of metal complexes with DNA [30]. DNA is known to offer several binding modes (outer-sphere non-covalent binding, metal coordination to nucleobases and phosphate backbone interactions) to the anticancer drugs [31]. The binding of intercalative ligand to DNA has been well characterized classically through absorption titration, following the hypochromism and red shift associated with the binding of the colored complex to the helix, due to the intercalative mode involving a strong stacking interaction between an aromatic chromophore and the DNA base pairs. The magnitudes of the hypochromism and red shift are commonly found to depend on the strength of the intercalative interaction [32].

The absorption spectra of the mixed oxalato complexes **1** and **5** in the presence or absence of DNA were mutually compared, which are shown in Fig. 1 and Fig. 2. In the UV region of the spectra, all the Cu(II) complexes exhibited an intense absorption around 331.0–386.4 nm and Zn(II) complexes showed bands in the region 322.5–339.3 nm (due to $n-\pi^*$ transition). With increasing concentration of DNA, both the ligands and their complexes showed hypochromicity and a red-shifted charge transfer peak maxima in the absorption spectra. The hypochromicity values of all the complexes observed in the presence of DNA were in the range 6.0–16.2%, and their red shifts in the region 2.0–6.2 nm. This feature might be ascribed to the fact that all the complexes could untwist the helix structure of DNA and made more bases embedding in DNA exposed [33,34]. The change in the absorbance values with increasing amount of DNA was used to evaluate the intrinsic binding constant K_b for the present complexes, the values of which are given in Table 2. The change in hypochromicity may be attributed to the nature of the binding of the complexes with DNA, which is significant due to π -stacking or hydrophobic interactions of the aromatic

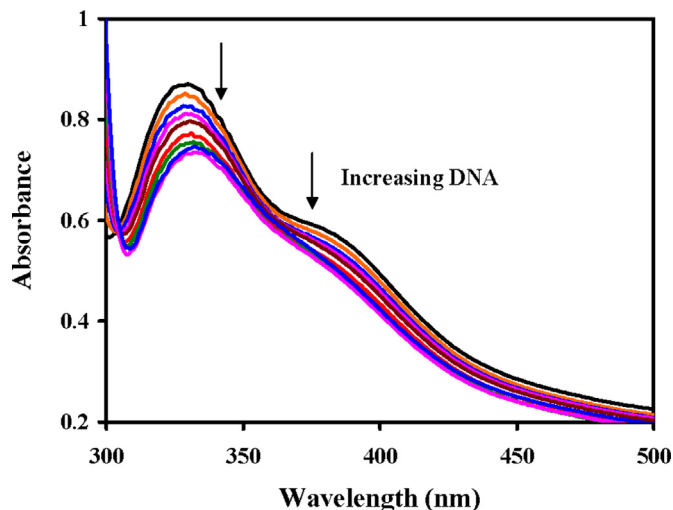


Fig. 1. Absorption spectrum of complex 1 in buffer pH = 7.2 at 25 °C in presence of increasing amount of DNA.

phenyl rings [35]. However, the metal ions play decisive role in DNA binding by these complexes. The binding strength of the synthesized complexes with DNA is shown as in the following order: $1 \approx 5 > 2 \approx 6 > 4 \approx 8 > 3 \approx 7$. The strong binding affinity of the metal complexes is due to additional π - π interaction through the aromatic phenyl rings and central metal ions which act as strong intercalators can greatly promote the DNA-binding ability of their complexes.

4.7.2. Viscosity measurements

To further confirm the interaction mode of the complexes with DNA, a viscosity study was carried out. As known, the viscosity of DNA is sensitive to changes occurring on the length of DNA helix mainly upon interaction of DNA with a compound. In the case of classic intercalation such as ethidium bromide [EB], the compound inserts in between the DNA base pairs leading to an increase in the separation of base pairs at intercalation sites in order to host the bound compound [36] and the length of the DNA helix and, subsequently, the DNA viscosity will exhibit an increase, which is usually proportional to the strength of the interaction. On the other

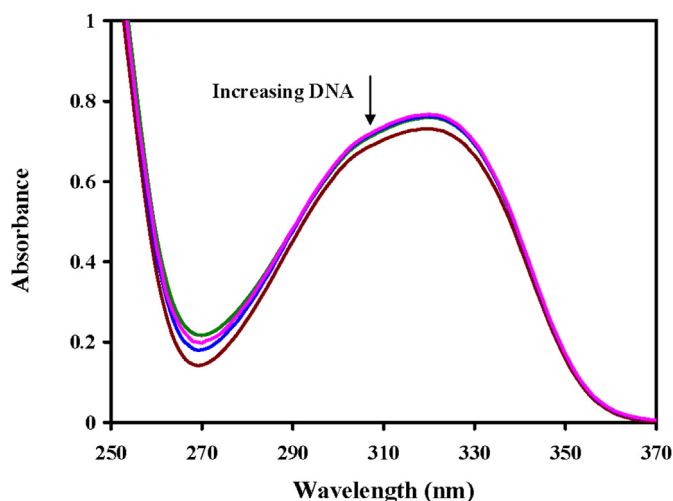


Fig. 2. Absorption spectrum of complex 5 in buffer pH = 7.2 at 25 °C in presence of increasing amount of DNA.

Table 2

Electronic absorption spectral properties of Cu(II) and Zn(II) mixed ligand complexes.

Complexes	λ_{\max} (nm)		$\Delta\lambda$ (nm)	$^a H\%$	$^b K_b$ (M^{-1})
	Free	Bound			
1	331.0	329.0	2.0	14.8	$2.3 \pm 0.05 \times 10^5$
	384.0	379.0	5.0	12.3	$2.0 \pm 0.07 \times 10^5$
2	351.5	354.5	3.0	8.5	$1.9 \pm 0.13 \times 10^4$
3	341.8	335.6	6.2	8.7	$1.2 \pm 0.04 \times 10^4$
4	386.4	384.3	2.1	6.0	$1.5 \pm 0.15 \times 10^4$
5	322.5	319.5	3.0	10.1	$1.8 \pm 0.03 \times 10^5$
6	320.6	315.4	5.2	16.2	$1.5 \pm 0.08 \times 10^4$
7	339.3	337.6	1.7	9.4	$1.3 \pm 0.14 \times 10^4$
8	329.5	331.5	2.0	6.1	$1.2 \pm 0.11 \times 10^4$

^a $H\% = [(A_{\text{free}} - A_{\text{bound}})/A_{\text{free}}] \times 100\%$.

^b K_b = Intrinsic DNA binding constant determined from the UV-Vis absorption spectral titration.

hand, in the existence of a partial and/or non-classic intercalation of a compound to DNA grooves, a bend or kink in the DNA helix should appear resulting in a slight reduce of its effective length with the DNA viscosity showing a slight decrease or remaining unchanged. The viscosity of the DNA solution increased with increasing ratio of the complexes to DNA. As expected, the known DNA-intercalator EB increased the relative viscosity of DNA due to its strong intercalation (Fig. 3). Compared with EB, complexes exhibit minor increase in the relative viscosity of CT-DNA, suggesting an intercalation mode between the complexes and DNA. This result further suggests an intercalating binding mode of the complexes with DNA and also parallels the above spectroscopic results, such as hypochromism and red shift of the complexes in the presence of DNA. The viscosity studies provide a strong evidence for intercalation. The information obtained from this study could be helpful to understand the mechanism of the interaction of small molecules with nucleic acids, and should be useful in the development of potential probes of DNA structure and conformation.

4.7.3. Electrochemical parameters

Cyclic voltammetry is one of the important and most popular electrochemical techniques for DNA binding studies with a fact that compound bound to DNA is redox active [37]. Electrochemical behavior of the synthesized complexes was investigated using cyclic voltammetric technique. The cyclic voltammetric experiment

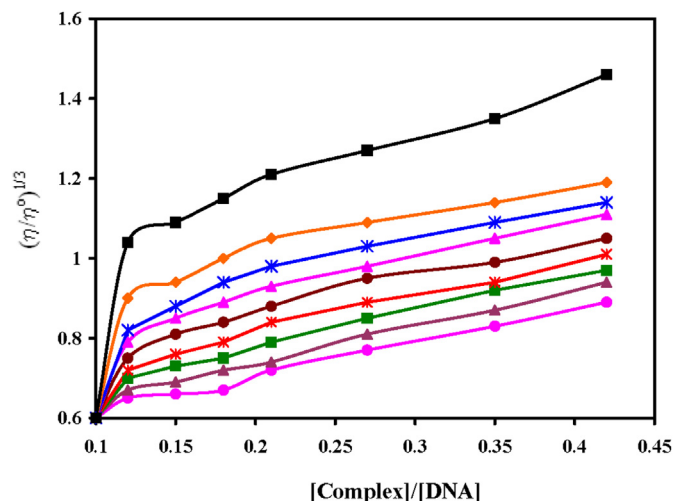


Fig. 3. Effect of increasing amounts of [EB] (■), 1 (♦), 2 (⋈), 3 (▲), 4 (●), 5 (⋈), 6 (■), 7 (▲) and 8 (●) on the relative viscosity of DNA. $1/R = [\text{Complex}]/[\text{DNA}]$ or $[\text{EB}]/[\text{DNA}]$.

was performed at room temperature in DMF using a glassy carbon working electrode a platinum counter electrode and an Ag/Ag⁺ reference electrode.

The voltammetric parameters obtained for all the complexes without and in the presence of DNA are given in Table 3. The cyclic voltammogram of the complex **1** in the absence and presence of different amounts of DNA are shown in Fig. 4. In the absence of CT DNA, the first redox cathodic peak appeared at 0.597 V for Cu(II) → Cu(I) ($E_{p_a} = 0.544$ V, $E_{p_c} = 0.597$ V, $\Delta E_p = -0.053$ V, and $E_{1/2} = 0.571$ V) and in the second redox couple, the cathodic peak appeared at 0.067 V for Cu(I) → Cu(0) ($E_{p_a} = 0.018$ V, $E_{p_c} = 0.067$ V, $\Delta E_p = -0.049$ V, and $E_{1/2} = 0.043$ V). The I_{p_c}/I_{p_a} ratios for these two redox couples are 1.43, and 0.78, respectively, which indicate that reaction of the complex on the glassy carbon electrode surface is a quasi-reversible redox process assignable to the Cu(II)/Cu(I) and Cu(I)/Cu(0) couple, as evidenced by the following criteria: (i) the peak-to-peak separation ΔE_p is greater than 49 mV, (ii) the current ratios I_{p_c}/I_{p_a} are constantly nearly equal to 1, and $E_{1/2} = [E_{p_c} + E_{p_a}]/2$ is found to be 0.571 V [38]. The voltammogram of the Zn(II) complex also shows quasi reversible process. The reason for the quasi-reversible electron transfer process may be due to slow electron transfer or the adsorption of the complex onto the electrode surface [39].

A quasi-reversible transfer process with the redox couple [Zn(II) → Zn(0)] was observed for the complexes **5–8**. The cathodic peak appeared at 1.057 V in the absence of DNA ($E_{p_a} = -0.461$ V, $E_{p_c} = 1.057$ V, $\Delta E_p = -1.517$ V, and $E_{1/2} = 0.301$ V). The I_{p_a}/I_{p_c} ratio is 0.93. This indicates the quasi-reversible redox process of the metal complexes. Incremental addition of DNA to the complex **5** resulted in a slight decrease in the current intensity and less negative shift of the oxidation peak potential. The resulting minor changes in the current and potential are indicative of diffusion of the metal complexes bound to the large, slowly diffusing DNA molecule [40].

4.8. Antimicrobial activity

The minimal inhibitory concentrations of tested compounds against certain bacteria and fungi are shown in Tables 4 and 5. The ligands (L¹–L⁴) and their metal complexes were prepared and tested for their *in vitro* antimicrobial activity against the five strains of bacteria (Gram negative and Gram positive), and five strains of fungi. Few metal complexes of the functionalized β -diketiminis showed high *in vitro* antimicrobial activity. All the mixed ligand metal complexes **1–8** showed significant antibacterial and antifungal activities compared to free ligands, but the activity was lesser than the standard drugs. Such increased activity of the complexes can be explained on the basis of Overtone's concept [41] and the Tweedy's Chelation theory [42]. The presence of electron-

Table 3
Redox potential profiles for interaction of DNA with Cu(II) and Zn(II) complexes.

Complexes	^a ΔE_p (V)		^b $E_{1/2}$ (V)		I_{p_c}/I_{p_a}
	Free	Bound	Free	Bound	
1	-0.053	-0.046	0.571	0.582	1.43
2	-0.064	-0.042	0.052	0.64	0.81
3	-0.112	-0.106	-0.173	-0.181	0.71
4	-0.122	-0.071	-0.231	-0.108	0.68
5	-1.517	-1.479	0.301	0.330	0.32
6	-0.121	0.254	-0.144	-0.131	3.28
7	0.119	0.199	-0.852	-0.942	6.18
8	0.174	0.168	-0.042	-0.051	0.79

Data from cyclic voltammetric measurements.

^a $\Delta E_p = E_{p_a} - E_{p_c}$.

^b $E_{1/2}$ is calculated as the average of anodic (E_{p_a}) and cathodic (E_{p_c}) peak potentials; $E_{1/2} = E_{p_a} + E_{p_c}/2$.

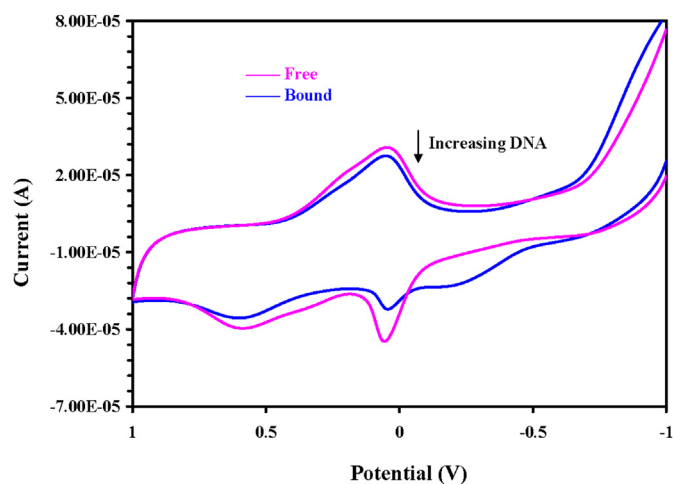


Fig. 4. Cyclic voltammogram of complex **1** in buffer pH = 7.2 at 25 °C in presence of increasing amount of DNA.

withdrawing nitro group on the aromatic ring increases the antimicrobial activities of the tested metal complexes compared to complexes having no substituent [43]. The nature of metal ion also plays a decisive role in determining antimicrobial properties. In the present study, the order of the antimicrobial activity of the synthesized compounds (based on the substituent present in the phenyl ring) is as follows: **1** \approx **5** > **4** \approx **8** > **3** \approx **7** > **2** \approx **6**. It is inferred from the results that electron-withdrawing nitro group has effective and direct impact on selective antimicrobial activities against both bacteria and fungi [44]. The mode of action of the compounds may involve the formation of a hydrogen bond through the azomethine group with the active centers of cell constituents, resulting in interferences with the normal cell process [45].

4.9. Interaction with pBR322 plasmid DNA

The intact double-stranded plasmid DNA exists in a compact circular closed conformation, the supercoiled DNA. If only one DNA strand is cleaved, the supercoiled DNA form assumes a more relaxed conformation known as "open circular DNA", which may be converted into linear DNA, following a cleavage event on the complementary strand near the first cleavage site. These three

Table 4
Minimum inhibitory concentration of the synthesized compounds against growth of bacteria (μ M).

Compound	Minimum inhibitory concentration (MIC) ($\times 10^4$ μ M) SEM = ± 2				
	<i>Staphylococcus aureus</i>	<i>Bacillus subtilis</i>	<i>Escherichia coli</i>	<i>Klebsiella pneumoniae</i>	<i>Salmonella typhi</i>
L ¹	16.7	16.1	15.3	16.7	16.3
L ²	17.0	18.2	16.3	16.4	16.8
L ³	19.3	10.9	18.7	18.3	17.1
L ⁴	18.5	19.6	17.0	17.6	17.9
1	9.6	10.1	8.7	8.3	9.8
2	10.6	11.9	10.9	10.2	11.3
3	10.3	11.4	10.3	9.6	11.0
4	10.0	10.1	9.4	9.1	10.4
5	11.1	11.4	12.4	11.5	13.3
6	13.6	13.3	13.6	13.3	14.3
7	12.7	11.9	13.3	12.1	14.3
8	12.3	11.7	12.9	12.3	14.1
^a Kanamycin	1.6	2.8	1.4	2.3	2.6

^a Kanamycin is used as the standard. The results obtained were the average of three replicates.

Table 5
Minimum inhibitory concentration of the synthesized compounds against the growth of fungi (μM).

Compound	Minimum inhibitory concentration (MIC) ($\times 10^4 \mu\text{M}$) SEM = ± 2				
	<i>Aspergillus niger</i>	<i>Fusarium solani</i>	<i>Curvularia lunata</i>	<i>Rhizoctonia bataticola</i>	<i>Candida albicans</i>
L ¹	16.2	17.4	15.5	14.9	16.4
L ²	18.9	18.5	17.6	15.8	17.6
L ³	20.3	21.6	19.5	17.5	18.4
L ⁴	19.2	19.0	18.1	16.9	17.9
1	10.1	12.1	12.3	13.6	14.2
2	14.9	16.7	14.9	16.9	16.1
3	14.1	16.1	14.1	15.1	14.9
4	12.0	14.4	13.4	14.3	14.4
5	13.7	15.1	13.4	16.3	16.9
6	18.4	17.1	16.9	17.4	12.6
7	15.2	16.9	15.4	17.1	16.5
8	14.1	16.3	14.1	16.3	16.1
^a Fluconazole	1.4	1.7	1.2	1.5	1.8

^a Fluconazole is used as the standard. The results obtained were the average of three replicates.

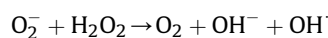
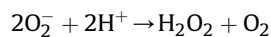
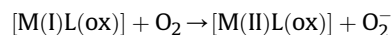
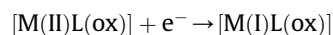
plasmid DNA conformations are distinguishable when subjected to agarose gel electrophoresis. The cleavage of plasmid pBR322 DNA induced by Cu(II) and Zn(II) complexes was performed in the absence of external cofactor agents (either oxidant or reductant). The Cu(II) complexes were found to promote the cleavage of plasmid pBR322 DNA from the supercoiled form (I) to the nicked form (II) and linear form (III) (Fig. 5(a)). No DNA cleavage was observed for the control in which the metal complex was absent (lane 1) and in presence of free CuCl₂ (100 μM). When the concentrations of the Cu(II) and Zn(II) complexes were increased (lanes 3–8), the amount of form I of pBR322 DNA diminished gradually, whereas the amounts of form II and III increased. These show, both the complexes are able to induce significant cleavage of the plasmid DNA at the concentration of 25 μM . At the concentration of 50 μM , Cu(II) and Zn(II) almost promote the complete conversion of DNA from form I to forms II and III.

In the presence of an oxidant (100 μM H₂O₂) under aerobic conditions (Fig. 5(b)), only 5 μM of Cu(II) and Zn(II) complexes can significantly cleave DNA. At highest concentration 50 μM the form I DNA has been fully depleted. This observation indicates that the chemical nuclease activity of the Cu(II) complex is significantly promoted with the addition of oxidants compared to Zn(II) complex. These observations support the hypothesis that Cu(II) and Zn(II) mixed ligand complexes most likely cleaved the plasmid DNA by a self-activating oxidative mechanism, which is similar to the manner in which bleomycin cooperates with a redox metal (Fe(II)) to trigger DNA cleavage without exogenous agents [46].

4.9.1. A mechanistic investigation of the DNA cleavage reaction

To explore the cleavage mechanism, the copper-mediated DNA cleavage was investigated with several different potential radical scavengers to identify the intermediate reactive oxygen species (ROS) in the absence of external cofactors (Fig. 5(c)). DMSO was used as hydroxyl radical (HO) scavenger; sodium azide was used as singlet oxygen (¹O₂) scavenger; and superoxide dismutase (SOD) was used as an O₂⁻ radical scavenger. The DNA breaks mediated by complexes **1–8** were not affected by the presence of the hydroxyl radical inhibitor DMSO, suggesting that diffusible hydroxyl radicals were not involved in the DNA damage mechanism. Addition of singlet oxygen scavenger NaN₃ revealed complete inhibition of nuclease (Fig. 5(c); lanes 4 and 5). These results suggested that ¹O₂ or any other singlet oxygen-like entity may participate in the DNA strand scission. On the other hand addition of SOD (Fig. 5(c); lanes 8 and 9) also showed comparatively little inhibitory effect on the DNA

cleavage. Based on the above observations we speculate that the complexes generated singlet oxygen and/or singlet oxygen like reactive oxygen species (ROS) which were responsible for nuclease activity. Considering that these types of active species mostly occur in oxidative cleavage, it is most likely that complexes **1–8** cleaved the DNA through a self-activating oxidative pathway. The possible redox mechanism between the metal complex and oxidant may be explained as follows:



To further test the involvement of H₂O₂ in the cleavage reaction, the analysis has been carried out under redox reaction conditions. The complexes **1–8** were found to form the same ROS involved in the reaction, and H₂O₂ was the crucial active intermediate involved in the DNA cleavage (Fig. 5(d)). Further, these complexes **1–8**, are capable of promoting DNA cleavage through an oxidative DNA damage pathway, in which giving active oxygen species such as singlet oxygen or singlet oxygen-like entity, probably a copper- peroxide, which cleaves DNA [47–49]. The resulting nuclease activity and mechanism under redox conditions strongly indicate a “self-activating” mechanism, which is most likely initiated by both the complexes through an oxidative pathway [50–52]. Further studies are currently underway to clarify the cleavage mechanism.

4.10. Cytotoxicity

Cytotoxicity is a common limitation in terms of the introduction of new compounds into the pharmaceutical industry. Schiff base complexes of copper have recently been investigated for their therapeutic potential [53] and the positive results obtained from DNA binding, cleavage and efficient microbial activity of the novel mixed-ligand complexes encouraged us to test their cytotoxicity against a panel of human cancer cell lines namely, human cervical cancer cell lines (HeLa) and human breast cancer cell lines (MCF-7) by colorimetric (MTT) assay in which mitochondrial dehydrogenase activity was measured as an indication of cell viability.

The IC₅₀ values have been calculated after 72 h of incubation with complexes and are listed in Table 6. As shown in Table 6, HeLa cells are more sensitive to complex **1** than MCF-7 cells, and the cytotoxicity of complex **1** against HeLa cells are higher compared with other complexes and cis-Pt(NH₃)₂Cl₂. Copper complexes inhibit the growth of HeLa cells in a dose-dependent manner (IC₅₀ = 0.50 μM). Although higher complex concentration reduces the percentages of cell survival, there is a significant difference in susceptibility between the complexes and cis-Pt(NH₃)₂Cl₂. Based on the results, we speculate that the better cytotoxic activity of the complexes **1–4** may be attributed to their stronger ability to cleave DNA. All the complexes are remarkable in displaying effective cytotoxicity against the HeLa human cervical cancer cell line and they are more potent than the widely used drug cisplatin.

The *in vitro* cytotoxicity against the animal tumor cell line (EAC) is also performed by trypan blue dye exclusion method. The IC₅₀ values of all the synthesized complexes are given in Table 6. This table shows that the complexes demonstrate different anti-tumor activities. Moreover, the results show excellent potential of complexes **1** and **4** towards EAC cell lines with IC₅₀ values (107.21 and 109.32 μM respectively), very sensitive with the value obtained for

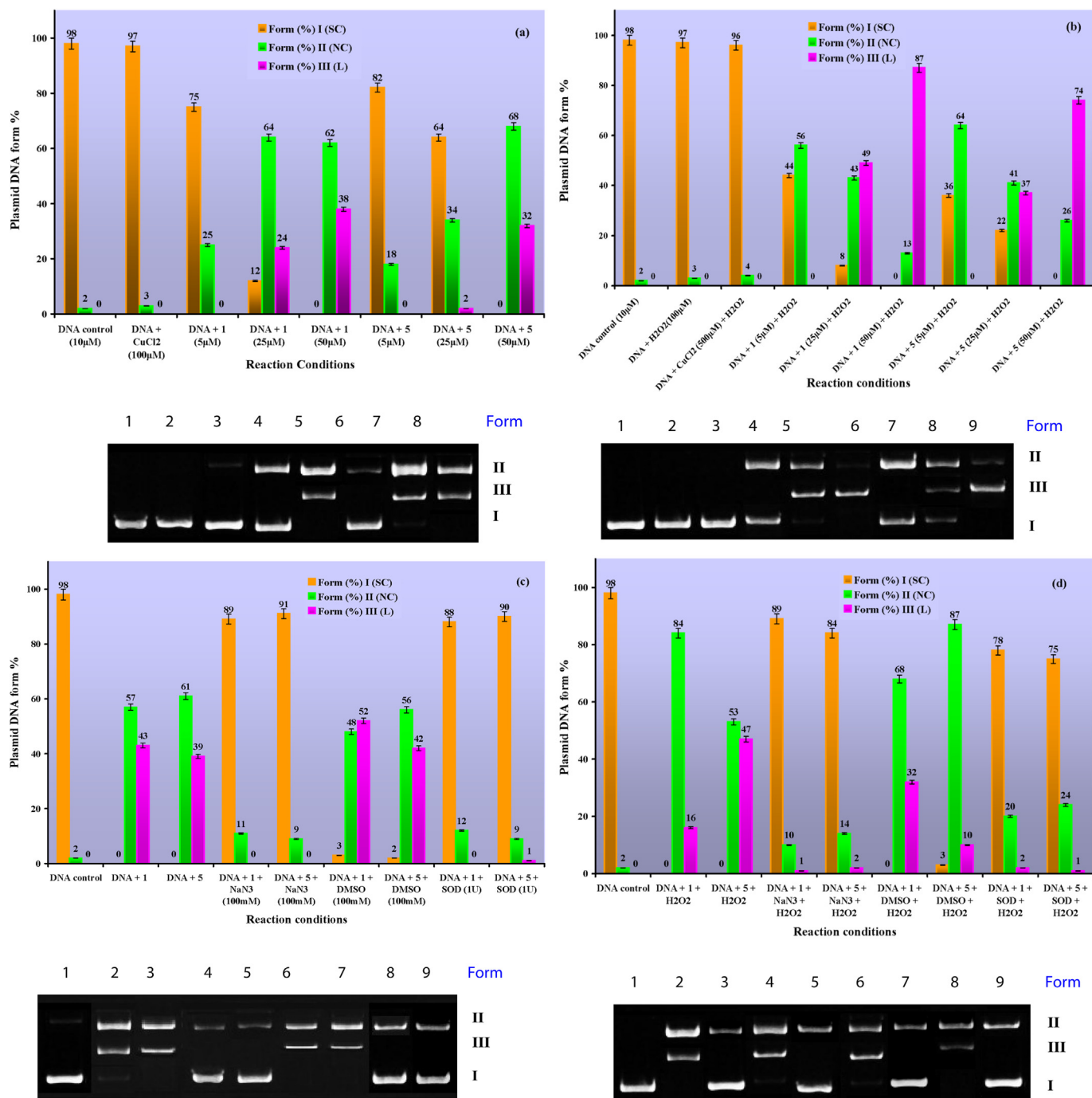


Fig. 5. (a) The gel electrophoresis of pBR322 DNA cleavage catalyzed by complex **1** and **5** in Tris–HCl buffer at 37 °C for 1.5 h with histogram of % cleavage forms. Lane 1: DNA control (10 µM); lane 2: DNA + CuCl₂ (100 µM); lanes 3–5: DNA + **5** (5, 25, 50 µM); lanes 6–8: DNA + **1** (5, 25, 50 µM). (b) The agarose gel electrophoresis of complexes **1** and **5** showing the oxidative cleavage of DNA (10 µM) with histogram of % cleavage forms. Lane 1: DNA control (10 µM); lane 2: DNA + H₂O₂; lane 3: DNA + CuCl₂ (500 µM) + H₂O₂; lanes 4–6: DNA + **1** (5, 25, 50 µM) + H₂O₂; lanes 7–9: DNA + **5** (5, 25, 50 µM) + H₂O₂. (c) The agarose gel electrophoresis of complexes **1** and **5** (50 µM) cleaving DNA (10 µM) in the presence of various radical scavengers under redox conditions for 1.5 h at 37 °C with histogram of % cleavage forms. Lane 1: DNA control; lanes 2 and 3: no inhibitor; complexes **1** and **5** (each 50 µM); lanes 4 and 5: complexes **1** and **5** + Na₃N (100 mM); lanes 6 and 7: complexes **1** and **5** + DMSO (100 mM); lanes 8 and 9: complexes **1** and **5** + SOD (1U). (d) The agarose gel electrophoresis of complexes **1** and **5** (50 µM) cleaving DNA (10 µM) in the presence of various radical scavengers for 1.5 h at 37 °C with histogram of % cleavage forms. Lane 1: DNA control; lane 2 and 6: no inhibitor; complexes **1** and **5** (each 50 µM) + H₂O₂; lane 3 and 7: **1** and **5** + Na₃N (100 mM) + H₂O₂; lane 4 and 8: **1** and **5** + DMSO (100 mM) + H₂O₂; lane 5 and 9: complexes **1** and **5** + SOD (1U) + H₂O₂.

the standard drug 5-Fluorouracil (5-FU), which is taken as positive control. It suggests that the β-diketimine moiety, bio-ligand and its metal ions have important effect on cytotoxicity. Amongst all the complexes tested, complex **1** has lowest IC₅₀ value of 107.21 µM. These results indicate that the complexes exert cytotoxic effects against tested carcinoma cell lines.

4.10.1. In vivo approach

Based on the above investigations, it is clearly demonstrated that the copper(II) complexes (**1**–**4**) exhibit superior *in vitro* biological responses. The *in vitro* cytotoxicity of EAC tumor cell lines show that the complexes **1** and **4** have lower IC₅₀ values which stimulated us to do the *in vivo* antitumor activity of EAC tumor

Table 6
IC₅₀ (μM) values of complexes and cis-platin against various cancer cell lines.

Compounds	IC ₅₀ (μM) SEM = ±0.5		
	HeLa	MCF-7	EAC
1	0.50	0.74	107.21
2	0.56	0.79	115.95
3	0.72	0.86	113.18
4	0.64	0.83	109.32
5	0.54	0.75	108.81
6	0.60	0.86	118.35
7	0.82	1.04	115.41
8	0.74	0.91	110.53
Cis-platin	0.53	0.72	–
5-FU	–	–	114.24

The results obtained were the average of three replicates from three determinations. IC₅₀, Drug concentration inhibiting 50% cellular growth following 72 h of drug exposure.

model. On the day 12, the biochemical and hematological parameters as regard to hemoglobin level, neutrophils and monocytes counts, were compared for the group treated with the standard drug 5-FU [54] and the same with the newly synthesized compound **1**. This shows the highest % of increase in life span over control on comparing the values obtained from normal and control groups. Hematological parameters of tumor-bearing mice on day 12 showed significant changes when compared to the normal mice (Table 7). From Table 7, differential count of WBC showed that the percentage of neutrophils increased ($P < 0.001$) while that of lymphocytes decreased ($P < 0.001$). At the same time interval, complexes (100 mg/kg/day, p.o.) treatment could change these altered parameters to almost normal.

The analysis of the hematological parameters showed minimum toxic effect in mice treated with complexes as compared with 5-FU [54]. After 12 days of transplantation, complexes were able to reverse the changes in the hematological parameters consequent to tumor inoculation. The present study revealed that the complexes were cytotoxic towards EAC. Fig. 6 shows smear showing matured EAC control cells (for 24 h) with definite cell wall and structure without degeneration. After EAC tumor cells treated with 5-FU, complex **4** for 24 h showing degenerative changes like membrane blebbing, vacuolated cytoplasm and low staining intensity for complex **1** with complete destruction of cells have efficient response than the complex **4** and compared to 5-FU. Interestingly, all the live normal cells upon treatment with the complexes **1–4** (Table 7) reveal that the complexes are non-toxic to normal cells (lymphocytes).

The effect of complexes **1** and **4** on the survival of tumor-bearing mice showed at dose of 100 μg/mL life span values 114.98 and 112.64% respectively (Table 8). The other complexes also showed

significant increase in the life span of the tumor bearing mice which were almost comparable with that of 5-FU.

5. Conclusion

Few novel mononuclear copper(II) and zinc(II) complexes (**1–8**) have been synthesized and characterized by physicochemical and spectroscopic methods. Characterizations of the new complexes have shown that, Cu(II) formed square planar complexes with 1:1:1 (metal:ligand) stoichiometry. The study of the interaction of complexes with CT-DNA has been investigated by absorption spectrophotometry, cyclic voltammetry and viscosity measurements. From the binding studies, it is evident that $1 \approx 5 > 2 \approx 6 > 4 \approx 8 > 3 \approx 7$ according to CT-DNA binding ability. In cyclic voltammetry, it is observed that there is positive shift of both the E_{pc} and E_{pa} along with the decrease of peak currents. The DNA interaction studies exhibit that all the complexes strongly interact with CT DNA by intercalative binding mode. Furthermore, the novel complexes exhibit good antimicrobial activity against the microbial strains, which may be due to the strong chelation and increased electron delocalization in increasing the lipophilic character of the metal ion into the cells in comparison to free ligands. These complexes could induce scission of pBR322 supercoiled DNA effectively without addition of external agents at pH = 7.2 and 37 °C. These results suggested that 1O_2 or any other singlet oxygen-like entity may participate in the DNA strand scission. The strong DNA binding ability coupled with the potent DNA cleavage activity shows that all the complexes might be capable of promoting DNA cleavage through an oxidative DNA damage pathway. In cytotoxicity experiment, complex **1** shows high *in vitro* cytotoxic property against HeLa/EAC cells compared to other complexes and cisplatin/5-FU. The above investigations clearly demonstrate that the complexes **1–4** exhibit superior *in vitro* biological responses. Further, the *in vivo* antitumor activity of complexes **1–4** against EAC tumor model in Adult Swiss female albino mice reveals that the complexes are non-toxic to normal cells (lymphocytes). Among them, complex **1** shows potential antitumor activity. Further studies are warranted to assess precise molecular mechanism of cytotoxicity and the pharmacological properties to elucidate the actual mechanism of the biological activity.

6. Experimental protocols

6.1. Reagents and instruments

All reagents, benzaldehyde, acetylacetone, *para* substituted anilines, oxalic acid and metal(II) chlorides were of Merck products and they were used as supplied. Commercial solvents were distilled

Table 7
Effect of Cu(II) complexes on hematological parameters of EAC tumor bearing mice.

Design of treatment	Hb (gm %)	RBC 10 ⁶ Cells/CU.MM	WBC 10 ³ Cells/CU.MM	Total protein mg%	PCV (%)	Differential count (%)		
						Lymphocytes	Neutrophils	Monocytes
Normal	12.92 ± 0.15	4.9 ± 0.12	6.78 ± 0.14	5.73 ± 0.26	16.86 ± 0.55	66.46 ± 1.36	32.6 ± 1.6	1.25 ± 0.45
Tumor control	5.78 ± 0.4 ^a	2.46 ± 0.14 ^a	18.74 ± 0.47 ^a	12.23 ± 0.34 ^a	25.98 ± 0.56 ^a	26.23 ± 1.16 ^a	72.8 ± 1.07 ^a	1.20 ± 0.45
1	12.13 ± 0.21 ^d	4.18 ± 0.19 ^d	15.58 ± 0.3 ^{a,d}	7.19 ± 0.17 ^{b,d}	17.14 ± 0.26 ^d	65.91 ± 0.86 ^d	35.12 ± 1.24 ^d	0.7 ± 0.45
2	11.39 ± 0.13 ^d	3.45 ± 0.15 ^{a,e}	14.95 ± 0.54 ^{a,d}	7.63 ± 0.27 ^{a,d}	16.98 ± 0.51 ^d	64.43 ± 1.0 ^d	31.60 ± 1.03 ^d	0.4 ± 0.24
3	11.04 ± 0.16 ^{a,d}	3.94 ± 0.13 ^{b,d}	12.16 ± 0.63 ^{a,d}	8.56 ± 0.17 ^{a,d}	17.18 ± 0.45 ^d	63.22 ± 1.28 ^d	36.27 ± 1.46 ^d	0.6 ± 0.42
4	13.07 ± 0.14 ^d	4.04 ± 0.15 ^d	11.47 ± 0.42 ^{a,d}	7.96 ± 0.41 ^{a,d}	19.98 ± 0.54 ^{b,d}	65.41 ± 1.21 ^d	38.54 ± 1.23 ^d	0.6 ± 0.27

^a $P < 0.001$.

^b $P < 0.01$.

^c $P < 0.05$ versus Normal.

^d $P < 0.001$.

^e $P < 0.01$ versus Tumor control. Data were analyzed by using one way ANOVA followed by Tukey–Kramer multiple comparison test.

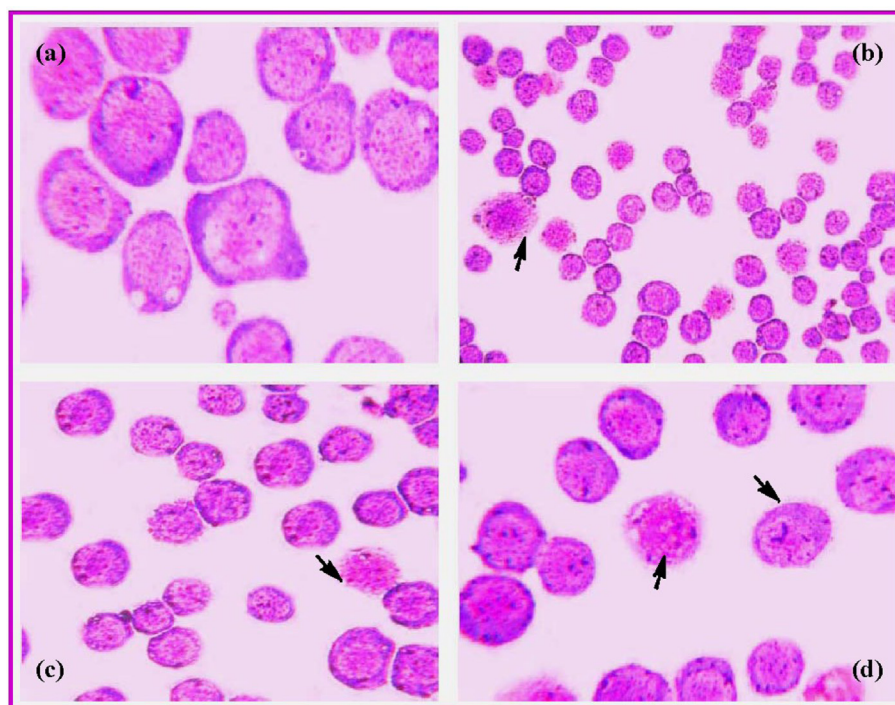


Fig. 6. (a) Smear showing matured EAC control cells (for 24 h) with definite cell wall and structure without degeneration. (b) EAC tumor cells treated with 5-FU for 24 h. (c) EAC tumor cells treated with complex **4** for 24 h. (d) complex **1** (for 24 h) treated with EAC cells showing degenerative changes like membrane blebbing, vacuolated cytoplasm and low staining intensity with complete destruction of cells.

and then used for the preparation of ligands and their complexes. DNA was purchased from Bangalore Genei (India). Microanalyses (C, H and N) were performed in Carlo Erba 1108 analyzer at Sophisticated Analytical Instrument Facility (SAIF), Central Drug Research Institute (CDRI), Lucknow, India. Molar conductivities in DMF (10^{-3} M) at room temperature were measured by using Systronic model-304 digital conductivity meter. Magnetic susceptibility measurement of the complexes was carried out by Gouy balance using copper sulfate pentahydrate as the calibrant. Infrared spectra ($4000\text{--}400\text{ cm}^{-1}$ KBr disc) of the samples were recorded on an IR Affinity-1 FT-IR Shimadzu spectrophotometer. NMR spectra were recorded on a Bruker Avance Dry 300 FT-NMR spectrometer in DMSO- d_6 , using TMS as the internal reference. EPR spectra were recorded on a Varian E 112 EPR spectrometer in DMSO solution both at room temperature (300 K) and liquid nitrogen temperature (77 K) using TCNE (tetracyanoethylene) as the g -marker. The absorption spectra were recorded by using Shimadzu model UV-1601 spectrophotometer at room temperature.

6.2. Synthesis of metal complexes

The Schiff base ligands were synthesized by the method reported in the literature by us [25]. To a stirred ethanolic solution of

Table 8
Effect of Cu(II) complexes treatment on the survival of tumor-bearing mice.

Treatment	MST	Increase in life span
Tumor control	16.26 ± 0.52	—
5- FU	$34.71 \pm 0.81^*$	140.67
1	$30.34 \pm 0.62^*$	114.98
2	$28.29 \pm 0.52^*$	111.85
3	$27.75 \pm 0.75^*$	108.14
4	$27.82 \pm 0.58^*$	112.64

$N = 6$; d of drug treatment = 9, $^*p < 0.01$ versus tumor control. Data were analyzed by one-way ANOVA followed by Dunnett's test.

the above Schiff base(s) (5 mmol), a solution of copper(II)/zinc(II) chloride (5 mmol) in ethanol was added dropwise. After the reaction for 1 h at 60°C , a solution of oxalic acid (5 mmol) in ethanol was added. The reaction solution was refluxed for 2 h. After cooling the reaction mixture to an ambient temperature, the formed solid was filtered, washed with diethyl ether and finally dried *in vacuum*.

[CuL¹(ox)] (**1**) Yield: 64%. Anal. Calc. for $\text{C}_{26}\text{H}_{20}\text{N}_4\text{O}_8\text{Cu}$: Cu, 11.0; C, 54.0; H, 3.5; N, 9.7; Found: Cu, 10.8; C, 53.6; H, 3.5; N, 9.5 (%). IR (KBr pellet, cm^{-1}): 1601 $\nu(\text{C}=\text{N})$; 1501 $\nu(\text{HC}=\text{C})$; 1471, 1304, 845 $\nu(\text{C}-\text{N str}; -\text{NO}_2)$; 1322 $\nu(\text{C}-\text{O})$; 1689 $\nu(\text{non-coordinated C}=\text{O in ox})$; 433 $\nu(\text{M}-\text{N})$, 508 $\nu(\text{M}-\text{O})$. MS m/z (%): 581 [M + 1]⁺. $\Delta_M 10^{-3}(\text{ohm}^{-1}\text{ cm}^2\text{ mol}^{-1}) = 8.6$. λ_{max} in DMF, 43,836, 35,225, 22,883. μ_{eff} (BM): 1.86.

[CuL²(ox)] (**2**) Yield: 62%. Anal. Calc. for $\text{C}_{26}\text{H}_{22}\text{N}_2\text{O}_4\text{Cu}$: Cu, 13.0; C, 64.0; H, 4.5; N, 5.7; Found: Cu, 12.9; C, 63.7; H, 4.5; N, 5.5 (%). IR (KBr pellet, cm^{-1}): 1605 $\nu(\text{C}=\text{N})$; 1505 $\nu(\text{HC}=\text{C})$; 1324 $\nu(\text{C}-\text{O})$; 1686 $\nu(\text{non-coordinated C}=\text{O in ox})$; 431 $\nu(\text{M}-\text{N})$, 505 $\nu(\text{M}-\text{O})$. MS m/z (%): 491 [M + 1]⁺. $\Delta_M 10^{-3}(\text{ohm}^{-1}\text{ cm}^2\text{ mol}^{-1}) = 8.9$. λ_{max} (cm^{-1}) in DMF, 40,475, 29,561, 23,041. μ_{eff} (BM): 1.88.

[CuL³(ox)] (**3**) Yield: 57%. Anal. Calc. for $\text{C}_{26}\text{H}_{22}\text{N}_2\text{O}_6\text{Cu}$: Cu, 12.2; C, 60.0; H, 4.2; N, 5.7; Found: Cu, 12.1; C, 59.8; H, 4.2; N, 5.6 (%). IR (KBr pellet, cm^{-1}): 1610 $\nu(\text{C}=\text{N})$; 1528 $\nu(\text{HC}=\text{C})$; 3428 $\nu(\text{OH})$; 1323 $\nu(\text{C}-\text{O})$; 1685 $\nu(\text{non-coordinated C}=\text{O in ox})$; 439 $\nu(\text{M}-\text{N})$, 526 $\nu(\text{M}-\text{O})$. MS m/z (%): 523 [M + 1]⁺. $\Delta_M 10^{-3}(\text{ohm}^{-1}\text{ cm}^2\text{ mol}^{-1}) = 8.3$. λ_{max} (cm^{-1}) in DMF, 41,326, 33,398, 23,201. μ_{eff} (BM): 1.87.

[CuL⁴(ox)] (**4**). Yield: 52%. Anal. Calc. for $\text{C}_{28}\text{H}_{26}\text{N}_2\text{O}_6\text{Cu}$: Cu, 11.5; C, 61.1; H, 4.8; N, 5.1; Found: Cu, 11.3; C, 61.0; H, 4.8; N, 5.0 (%). IR (KBr pellet, cm^{-1}): 1607 $\nu(\text{C}=\text{N})$; 1537 $\nu(\text{HC}=\text{C})$; 1270, 1083, $\nu(\text{C}-\text{O}-\text{C}-)$; 1321 $\nu(\text{C}-\text{O})$; 1689 $\nu(\text{non-coordinated C}=\text{O in ox})$; 445 $\nu(\text{M}-\text{N})$, 531 $\nu(\text{M}-\text{O})$. MS m/z (%): 551 [M + 1]⁺. $\Delta_M 10^{-3}(\text{ohm}^{-1}\text{ cm}^2\text{ mol}^{-1}) = 9.1$. λ_{max} (cm^{-1}) in DMF, 41,689, 31,626, 23,364. μ_{eff} (BM): 1.84.

[ZnL¹(ox)] (**5**) Yield: 61%. Anal. Calc. for $\text{C}_{26}\text{H}_{20}\text{N}_4\text{O}_8\text{Zn}$: Zn, 12.0; C, 56.4; H, 3.6; N, 5.1; Found: Zn, 11.8; C, 56.3; H, 3.6; N, 5.0 (%). IR

(KBr pellet, cm^{-1}): 1612 $\nu(\text{C}=\text{N})$; 1503 $\nu(\text{HC}=\text{C})$; 1467, 1307, 835 $\nu(\text{C}-\text{N}$ str; $-\text{NO}_2$); 1323 $\nu(\text{C}-\text{O})$; 1681 $\nu(\text{non-coordinated C}=\text{O}$ in ox). 448 $\nu(\text{M}-\text{N})$, 509 $\nu(\text{M}-\text{O})$. ^1H NMR (δ): (aromatic) 6.9–7.4 (m); ($-\text{CH}_3$, 6H), 2.1 (s). ^{13}C NMR (δ): 124.6–126.4 (C_1 to C_3), 134.3 (C_4), 136.1 (C_5), 114.3 (C_6), 170.4 (C_7), 20.4 (C_8), 153.1 (C_9), 123.3 (C_{10}), 124.6 (C_{11}), 146.6 (C_{12}), 164.5 (C_{13}). MS m/z (%): 582 $[\text{M} + 1]^+$. $\Delta_M 10^{-3} (\text{ohm}^{-1} \text{cm}^2 \text{mol}^{-1}) = 13.6$. $\lambda_{\text{max}} (\text{cm}^{-1})$ in DMF, 42,359, 32,161. μ_{eff} (BM): diamagnetic.

$[\text{ZnL}^2(\text{ox})]$ (6) Yield: 59%. Anal. Calc. for $\text{C}_{26}\text{H}_{22}\text{N}_2\text{O}_4\text{Zn}$: Zn, 13.3; C, 63.5; H, 4.5; N, 5.7; Found: Zn, 13.1; C, 63.3; H, 4.4; N, 5.4 (%). IR (KBr pellet, cm^{-1}): 1606 $\nu(\text{C}=\text{N})$; 1526 $\nu(\text{HC}=\text{C})$; 1320 $\nu(\text{C}-\text{O})$; 1685 $\nu(\text{non-coordinated C}=\text{O}$ in ox). 441 $\nu(\text{M}-\text{N})$, 517 $\nu(\text{M}-\text{O})$. ^1H NMR (δ , ppm): (aromatic) 6.9–7.3 (m); ($-\text{CH}_3$, 6H), 2.2 (s). ^{13}C NMR (δ , ppm): 125.3–128.6 (C_1 to C_3), 133.1 (C_4), 136.4 (C_5), 112.3 (C_6), 166.5 (C_7), 20.4 (C_8), 136.9 (C_9), 119.4 (C_{10}), 131.6 (C_{11}), 128.3 (C_{12}), 168.7 (C_{13}). MS m/z (%): 492 $[\text{M} + 1]^+$. $\Delta_M 10^{-3} (\text{ohm}^{-1} \text{cm}^2 \text{mol}^{-1}) = 12.1$. $\lambda_{\text{max}} (\text{cm}^{-1})$ in DMF, 40,561, 29,198. μ_{eff} (BM): diamagnetic.

$[\text{ZnL}^3(\text{ox})]$ (7). Yield: 53%. Anal. Calc. for $\text{C}_{26}\text{H}_{22}\text{N}_2\text{O}_6\text{Zn}$: Zn, 12.5; C, 59.6; H, 4.2; N, 5.4; Found: Zn, 12.2; C, 59.4; H, 4.2; N, 5.3 (%). IR (KBr pellet, cm^{-1}): 1615 $\nu(\text{C}=\text{N})$; 1524 $\nu(\text{HC}=\text{C})$; 3428 $\nu(\text{OH})$; 1322 $\nu(\text{C}-\text{O})$; 1684 $\nu(\text{non-coordinated C}=\text{O}$ in ox). 430 $\nu(\text{M}-\text{N})$, 513 $\nu(\text{M}-\text{O})$. ^1H NMR (δ , ppm): (aromatic) 6.8–7.2 (m); ($-\text{OH}$, 1H) 10.3 (s); ($-\text{CH}_3$, 6H), 2.4 (s). ^{13}C NMR (δ , ppm): 125.0–127.9 (C_1 to C_3), 134.4 (C_4), 136.3 (C_5), 114.5 (C_6), 169.3 (C_7), 20.3 (C_8), 147.2 (C_9), 122.9 (C_{10}), 118.4 (C_{11}), 154.6 (C_{12}), 164.7 (C_{13}). MS m/z (%): 524 $[\text{M} + 1]^+$. $\Delta_M 10^{-3} (\text{ohm}^{-1} \text{cm}^2 \text{mol}^{-1}) = 15.2$. $\lambda_{\text{max}} (\text{cm}^{-1})$ in DMF, 41,741, 33,853. μ_{eff} (BM): diamagnetic.

$[\text{ZnL}^4(\text{ox})]$ (8) Yield: 51%. Anal. Calc. for $\text{C}_{28}\text{H}_{26}\text{N}_2\text{O}_6\text{Zn}$: Zn, 12.0; C, 61.0; H, 5.0; N, 5.1; Found: Zn, 11.8; C, 60.8; H, 5.0; N, 4.9 (%). IR (KBr pellet, cm^{-1}): 1611 $\nu(\text{C}=\text{N})$; 1543 $\nu(\text{HC}=\text{C})$; 1264, 1081, $\nu(\text{C}-\text{O}-\text{C})$; 1326 $\nu(\text{C}-\text{O})$; 1683 $\nu(\text{non-coordinated C}=\text{O}$ in ox). 436 $\nu(\text{M}-\text{N})$, 533 $\nu(\text{M}-\text{O})$. ^1H NMR (δ): (aromatic) 6.8–7.3 (m); ($-\text{CH}_3$, 6H), 2.2 (s); 3.7 ($-\text{OCH}_3$, 6H). ^{13}C NMR (δ): 124.9–128.6 (C_1 to C_3), 132.5 (C_4), 137.5 (C_5), 112.8 (C_6), 168.2 (C_7), 20.3 (C_8), 142.1 (C_9), 122.2 (C_{10}), 116.1 (C_{11}), 158.4 (C_{12}), 58.3 (C_{13}), 164.3 (C_{14}). MS m/z (%): 552 $[\text{M} + 1]^+$. $\Delta_M 10^{-3} (\text{ohm}^{-1} \text{cm}^2 \text{mol}^{-1}) = 12.8$. $\lambda_{\text{max}} (\text{cm}^{-1})$ in DMF, 42,359, 31,833. μ_{eff} (BM): diamagnetic.

6.3. DNA binding experiments

The interaction between metal complexes and DNA was studied using electronic absorption, viscosity and electrochemical methods. Disodium salt of calf thymus DNA was stored at 4 °C. All the experiments involving the interaction of the complexes with calf thymus (CT) DNA were carried out in Tris–HCl buffer (50 mM Tris–HCl, pH 7.2) containing 5% DMF at room temperature. A solution of CT DNA in the buffer gave a ratio of UV absorbance at 260 and 280 nm of about 1.8–1.9, indicating that the CT DNA was sufficiently free from protein [55]. The concentration of DNA was measured by using its extinction coefficient at 260 nm ($6600 \text{ M}^{-1} \text{cm}^{-1}$) after 1: 100 dilution. Stock solutions were stored at 4 °C and used not more than 4 days. Doubly distilled water was used to prepare solutions. Concentrated stock solutions of the complexes were prepared by dissolving the complexes in DMF and diluting properly with the corresponding buffer to the required concentration for all the experiments.

Absorption titration experiment was performed by keeping the concentration of the metal complex as constant at 50 μM while varying the concentration of the CT DNA within 40–400 μM . While measuring the absorption spectrum, equal quantity of CT DNA was added to both the complex solution and the reference solution to eliminate the absorbance of CT DNA itself. From the absorption data, the intrinsic binding constant (K_b) was determined from the plot of $[\text{DNA}]/(\epsilon_a - \epsilon_f)$ versus $[\text{DNA}]$ using the following equation (1):

$$[\text{DNA}]/(\epsilon_a - \epsilon_f) = [\text{DNA}]/(\epsilon_b - \epsilon_f) + [K_b(\epsilon_b - \epsilon_f)]^{-1} \quad (1)$$

where $[\text{DNA}]$ is the concentration of CT DNA in base pairs. The apparent absorption coefficients ϵ_a , ϵ_f and ϵ_b correspond to $A_{\text{obs}}/[\text{M}]$, the extinction coefficient for the free metal(II) complex and extinction coefficient for the metal(II) complex in the fully bound form, respectively [56]. K_b is given by the ratio of slope to the intercept.

Cyclic voltammetry studies were performed on a CHI 620C electrochemical analyzer with three electrode system of glassy carbon as the working electrode, a platinum wire as auxiliary electrode and Ag/AgCl as the reference electrode. Solutions were deoxygenated by purging with N_2 prior to measurements. Viscosity experiments were carried on an Ostwald viscometer, immersed in a thermostated water-bath maintained at a constant temperature at 30.0 ± 0.1 °C. CT DNA samples of approximately 0.5 mM were prepared by sonicating in order to minimize complexities arising from CT DNA flexibility [57]. Flow time was measured with a digital stopwatch three times for each sample and an average flow time was calculated. Data were presented as $(\eta/\eta_0)^{1/3}$ versus the concentration of the metal(II) complexes, where η is the viscosity of CT DNA solution in the presence of complex, and η_0 is the viscosity of CT DNA solution in the absence of complex. Viscosity values were calculated after correcting the flow time of buffer alone (t_0), $\eta = (t - t_0)/t_0$ [58].

6.4. Interaction with pBR322 plasmid DNA

The extent of pBR322 DNA cleavage in the absence and presence of an activating agents H_2O_2 and various radical scavengers like sodium azide (singlet oxygen), SOD (superoxide) DMSO (Hydroxyl radical scavenger) was monitored using agarose gel electrophoresis. In reactions using supercoiled pBR322 plasmid DNA form I (2 μM , 10 μM) in Tris–HCl buffer (50 mM) with 50 mM NaCl (pH 7.2) which was treated with the metal complex (5–50 μM) and activating agents (100 μM) followed by dilution with the Tris–HCl buffer to a total volume of 20 μL . The samples were incubated for 1 h at 37 °C. A loading buffer containing 25% bromophenol blue, 0.35% xylene cyanol, 30% glycerol (3 μM) was added and electrophoresis was performed at 40 V for each hour in Tris–Acetate–EDTA (TAE) buffer using 1% agarose gel containing 1 μM ethidium bromide. The cleavage efficiency was measured by determining the ability of the complex to convert the supercoiled form I DNA to nicked circular form II and linear form III. After staining with an EB solution (1 μM), the bands visualized and photographed. The extent of DNA form I cleavage was measured from the intensities of the bands using UVITEC Gel Documentation System. The observed error in measuring the band intensities was ~4%. Inhibition reactions were carried out by prior incubation of the SC pBR322 DNA (10 μM) with DMSO (2 μM).

6.5. Evaluation of antimicrobial activity

Qualitative determination of antimicrobial activity was done using the disc diffusion method. The biological activities of synthesized Schiff bases and their metal complexes were studied for their antibacterial and antifungal activities in DMF solvent against bacterial and fungal species. Suspensions in sterile peptone water from 24 h cultures of microorganisms were adjusted to 0.5 McFarland. Muller–Hinton petri discs of 90 mm were inoculated using these suspensions. Paper discs (6 mm in diameter) containing 10 μL of the substance to be tested were placed in a circular pattern in each inoculated plate. DMF impregnated discs were used as negative controls. Toxicity tests of the solvent, DMF, showed that

the concentration used in antibacterial activity assays did not interfere with the growth of the microorganisms.

6.5.1. Determination of MIC

The *in vitro* antimicrobial activity was performed against Gram-positive bacteria: *Staphylococcus aureus*, *Bacillus subtilis* and *Salmonella typhi* Gram-negative bacteria: *Escherichia coli*, *Pseudomonas aeruginosa* and fungal strains: *Rhizoctonia bataticola*, *Fusarium Solani*, *Candida albicans*, *Culvularia lunata* and *Aspergillus niger*. The standard and test samples were dissolved in DMF to give a concentration of 100 μM . The minimum inhibitory concentration (MIC) was determined by broth microdilution method [59]. Dilutions of test and standard compounds were prepared in nutrient broth (bacteria) or Sabouraud dextrose broth (fungi) [60]. The samples were incubated at 37 °C for 24 h (bacteria) and at 25 °C for 48 h (fungi), respectively, and the results were recorded in terms of MIC (the lowest concentration of test substance which inhibited the growth of microorganisms).

6.6. Antitumor studies

Adult Swiss female albino mice (20–25 g) were procured from Animal house, Vivekananda College of Pharmacy, Tiruchengode, Tamil Nadu, India and used throughout the study. They were housed in microton boxes in controlled environment (temperature 25 ± 2 °C and 12 h dark/light cycle) with standard laboratory diet and water *ad libitum*. The experiments were performed in accordance with guidelines established by the European community for the care and use of laboratory animals, and were approved by the Institutional Animal Ethics Committee (IAEC) of Vivekananda College of Pharmacy, Tamil Nadu, India.

6.6.1. Cells

Ehrlich Ascites Carcinoma (EAC) cells were obtained through the courtesy of Amala Cancer Research Centre, Trissur, India. They were maintained by weekly intraperitoneal inoculation of 10⁶ cells/mouse [61].

6.6.2. Mean survival time [62]

Animals were inoculated with 1×10^6 cells/mouse on day '0' and treatment with synthesized complexes started 24 h after inoculation, at a dose of 100 mg/kg/day, p.o. The control group was treated with the same volume of 0.9% sodium chloride solution. All the treatments were given for nine days. The median survival time (MST) of each group, consisting of 10 mice was noted. The anti-tumor efficacy of complexes was compared with that of 5-fluorouracil (Dabur Pharmaceutical Ltd, India; 5-FU, 20 mg/kg/day, i.p. for 9 days).

6.6.3. Hematological parameters [62]

The hematological parameters like total red blood cell (RBC), white blood cells (WBC), lymphocytes (LYM), hematocrit (HCT), hemoglobin (HGB) and MID cells (less frequently occurring and rare cells correlating to monocytes, eosinophils, basophils etc.) were determined using a blood automatic analyzer (CellDYN, Abbot Inc. USA). In order to detect the influence of complexes on the hematological status of EAC-bearing mice, a comparison was made among three groups ($n = 5$) of mice on the 14th day after inoculation. The groups comprised of (1) tumor-bearing mice (2) tumor-bearing mice treated with complexes (100 mg/kg/day, p.o. for the first 9 days) and (3) control mice (normal). Blood was drawn from each mouse by the retro orbital plexus method and the white blood cell count (WBC), red blood cell count (RBC), hemoglobin and protein were determined [63–65].

6.6.4. Cytotoxicity

Human cervical cancer cell lines (HeLa) and Human breast cancer (MCF-7) cells were obtained from National Centre for Cell Science (Pune, India). Stock cells of HeLa and MCF-7 cell lines were cultured in RPMI-1640 or DMEM supplemented with 10% inactivated new born calf serum, penicillin (100 IU/mL), streptomycin (100 μM), and amphotericin-B (5 μM) under a humidified atmosphere of 5% CO₂ at 37 °C until confluent. The cells were dissociated in 0.2% trypsin, 0.02% EDTA in phosphate buffer saline solution. The stock culture was grown in 25 cm² tissue-culture flasks, and cytotoxicity experiments were carried out in 96-well microtiter plates (Tarsons India, Kolkata, India).

Cell lines in the exponential growth phase were washed, trypsinized and resuspended in complete culture media. Cells were plated at 10,000 cells/well in 96-well microtiter plates and incubated for 24 h, during which a partial monolayer formed. They were then exposed to various concentrations of the complexes (0.1–100 μM) and cisplatin. Control wells received only maintenance medium. The plates were incubated at 37 °C in a humidified incubator with 5% CO₂ for a period of 72 h at the end of 72 h, viability was determined by MTT assay.

6.6.5. Effect of Cu(II) and Zn(II) complexes on *in vitro* cytotoxicity

Short-term cytotoxicity was assessed by incubating 1×10^6 EAC cells in 1 mL phosphate buffer saline with varying concentrations of the complexes at 37 °C for 3 h in CO₂ atmosphere ensured using a McIntosh field jar. The viability of the cells was determined by the trypan blue exclusion method [66].

Acknowledgments

The authors express their heartfelt thanks to the Science & Engineering Research Board (SERB), DST, New Delhi (File No.SR/S1/IC-27/2012) for financial support. They also express their gratitude to the College Managing Board, Principal and Head of the Department of Chemistry, VHNSN College, Virudhunagar for providing research facilities. They thank Prof. R. Senthil Kumar, Department of Pharmaceutical Chemistry, Swami Vivekananda College of Pharmacy, Elayampalayam, Tiruchengode, for *in vitro* and *in vivo* anti-cancer studies.

Appendix A. Supplementary data

Supplementary data related to this article can be found at <http://dx.doi.org/10.1016/j.ejmech.2014.04.032>.

References

- [1] G.J. Kelloff, Perspective on cancer chemoprevention research and drug development, *Advances in Cancer Research* 78 (2000) 199–344.
- [2] N.J. Wheate, S. Walker, G.E. Craig, R. Oun, The status of platinum anticancer drugs in the clinic and in clinical trials, *Dalton Transactions: An International Journal of Inorganic Chemistry* 39 (2010) 8113–8127.
- [3] L. Kelland, The resurgence of platinum-based cancer chemotherapy, *Nature Reviews. Cancer* 7 (2007) 573–584.
- [4] D. Lebowitz, R. Canetta, Clinical development of platinum complexes in cancer therapy: an historical perspective and an update, *European Journal of Cancer: Official Journal for European Organization for Research and Treatment of Cancer (EORTC) [and] European Association for Cancer Research (EACR)* 34 (1998) 1522–1534.
- [5] A. Djekovic, B. Petrovic, Z.D. Bugarcic, R. Puchta, R.V. Eldik, Kinetics and mechanism of the reactions of Au(III) complexes with some biologically relevant molecules, *Dalton Transactions: An International Journal of Inorganic Chemistry* 40 (2012) 3633–3641.
- [6] P.C. Bruijninx, P.J. Sadler, New trends for metal complexes with anticancer activity, *Current Opinion in Chemical Biology* 12 (2008) 197–206.
- [7] (a) I. Ott, R. Gust, Non platinum metal complexes as anti-cancer drugs, *Archiv der Pharmazie* 340 (2007) 117–126;
(b) S. Rafique, M. Idrees, A. Nasim, H. Akbar, A. Athar, *Transition metal*

- complexes as potential therapeutic agents, *Biotechnology and Molecular Biology Reviews* 5 (2010) 38–45.
- [8] F. Mancin, P. Scrimin, P. Tecilla, U. Tonellato, Artificial nucleases, *Chemical Communications* (2005) 2540–2548.
- [9] R. Pitie, C.J. Burrows, B. Meunier, Mechanisms of DNA cleavage by copper complexes of 3-clip-phen and of its conjugate with a distamycin analog, *Nucleic Acids Research* 28 (2000) 4856–4858.
- [10] B. Maity, M. Roy, S. Saha, A.R. Chakravarty, Photoinduced DNA and protein cleavage activity of ferrocene-conjugated ternary copper(II) complexes, *Organometallics* 28 (2009) 1495–1505.
- [11] A. Sreedhara, J.A. Cowan, Catalytic hydrolysis of DNA by metal complexes, *Journal of Biological Inorganic Chemistry: JBIC: a Publication of the Society of Biological Inorganic Chemistry* 6 (2001) 337–347.
- [12] P. Kumar, S. Gorai, M.K. Santra, B. Mondal, D. Manna, DNA binding, nuclease activity and cytotoxicity studies of Cu(II) complexes of tridentate ligands, *Dalton Transactions: An International Journal of Inorganic Chemistry* 41 (2012) 7573–7581.
- [13] R. Karvembu, K. Natarajan, Synthesis and spectral studies of binuclear ruthenium(II) carbonyl complexes containing bis(β -diketone) and their applications, *Polyhedron* 21 (2002) 219–223.
- [14] H. Zeng, J. Xie, P.G. Schultz, Genetic introduction of a diketone-containing amino acid into proteins, *Bioorganic & Medicinal Chemistry Letters* 16 (2006) 5356–5359.
- [15] N. Raman, R. Jeyamurugan, R. Senthilkumar, B. Rajkapoor, S.G. Franzblau, In vivo and in vitro evaluation of highly specific thiolate carrier group copper(II) and zinc(II) complexes on Ehrlich ascites carcinoma tumor model, *European Journal of Medicinal Chemistry* 45 (2010) 5438–5451.
- [16] S. Sumathi, P. Tharmaraj, C.D. Sheela, C. Anitha, Synthesis and studies on Cu(II), Co(II), Ni(II) complexes of Knoevenagel β -diketone ligands, *Spectrochimica Acta Part A* 97A (2012) 377–383.
- [17] R.S. Sancheti, R.S. Bendre, A.A. Kumbhar, Cu(II), Ni(II), Zn(II) and Fe(III) complexes containing a N_2O_2 donor ligand: synthesis, characterization, DNA cleavage studies and crystal structure of [Cu(HL)Cl], *Polyhedron* 31 (2012) 12–18.
- [18] Q. Wang, Z. Yu, Q. Wang, W. Li, F. Gao, S. Li, Synthesis, crystal structure and DNA-binding properties of a mononuclear copper complex with pyridine-2-carboxylate ligand, *Inorganica Chimica Acta* 383 (2012) 230–234.
- [19] B. Zhao, P. Cheng, X.Y. Cheng, C. Cheng, W. Shi, D.Z. Liao, S.P. Yan, Z.H. Jiang, Design and synthesis of 3d-4f metal based zeolite-type materials with a 3D nanotubular structure encapsulated "water" pipe, *Journal of the American Chemical Society* 126 (2004) 3012–3013.
- [20] X.L. Wang, C. Qin, E.B. Wang, Y.G. Li, C.W. Hu, L. Xu, Designed double layer assembly: a three-dimensional open framework with two types of cavities by connection of infinite two-dimensional bilayer, *Chemical Communications* 4 (2004) 378–379.
- [21] E.J. Gao, T.D. Sun, S.H. Liu, S. Ma, Z. Wen, Y. Wang, M.C. Zhu, L. Wang, X.N. Gao, F. Guan, M.J. Guo, F.C. Liu, Synthesis, characterization, interaction with DNA and cytotoxicity in vitro of novel pyridine complexes with Zn(II), *European Journal of Medicinal Chemistry* 45 (2010) 4531–4538.
- [22] O. Castillo, I. Muga, A. Luque, Juan M.G. Zorrilla, J. Sertucha, P. Vitoria, P. Roman, Synthesis, chemical characterization, X-ray crystal structure and magnetic properties of oxalato-bridged copper(II) binuclear complexes with 2,2'-bipyridine and diethylenetriamine as peripheral ligands, *Polyhedron* 18 (1999) 1235–1245.
- [23] X. Feng, L.Y. Wang, J.S. Zhao, J.G. Wang, N.S. Weng, B. Liu, X.G. Shi, Series of anion-directed lanthanide-rigid-flexible frameworks: syntheses, structures, luminescence and magnetic properties, *Crystal Engineering Communications* 12 (2010) 774–783.
- [24] X. Feng, J.S. Zhao, L.Y. Wang, X.G. Shi, An anion-directed unprecedented three-dimensional array with erbium(III) based on the 2,6-pyridinedicarboxylate, *Inorganic Chemistry Communications* 12 (2009) 388–391.
- [25] N. Raman, N. Pravin, Lasing the DNA fragments through β -diketimine framed Knoevenagel condensed Cu(II) and Zn(II) complexes – an *in vitro* and *in vivo* approach, *Spectrochimica Acta. Part A, Molecular and Biomolecular Spectroscopy* 118 (2014) 867–882.
- [26] K. Nakamoto, *Infrared and Raman Spectra of Inorganic and Coordination Compounds*, fourth ed., Wiley, New York, 1986.
- [27] A.B.P. Lever, *Inorganic Electronic Spectroscopy*, Elsevier, Amsterdam, 1984.
- [28] A.W. Addison, Is ligand topology an influence on the redox potentials of copper complexes? *Inorganica Chimica Acta* 162 (1989) 217–220.
- [29] R.K. Ray, G.B. Kauffman, EPR spectra and covalency of bis(amidino-urea/O-alkyl-1-amidino-urea)copper(II) complexes part II. Properties of the CuN_4^{2-} chromophore, *Inorganica Chimica Acta* 173 (1990) 207–214.
- [30] S.A. Tysoe, R.J. Morgan, A.D. Baker, T.C. Streckas, Spectroscopic investigation of differential binding modes of DELTA and LAMBDA-Ru(bpy)₂(ppz)₂²⁺ with calf thymus DNA, *The Journal of Physical Chemistry* 97 (1993) 1707–1711.
- [31] S. Mathur, S. Tabassum, Template synthesis of novel carboxamide dinuclear copper (II) complex: spectral characterization and reactivity towards calf-thymus DNA, *Biometals: An International Journal on the Role of Metal Ions in Biology, Biochemistry, and Medicine* 21 (2008) 299–310.
- [32] A.M. Pyle, J.P. Rehmann, R. Meshoyrer, C.V. Kumar, N.J. Turro, J.K. Barton, Mixed-ligand complexes of ruthenium(II): factors governing binding to DNA, *Journal of the American Chemical Society* 111 (1989) 3051–3059.
- [33] Q.L. Zhang, J.G. Liu, H. Xu, H. Li, J.Z. Liu, H. Zhou, L.H. Qu, L.N. Ji, Synthesis, characterization and DNA-binding studies of cobalt(III) polypyridyl complexes, *Polyhedron* 20 (2001) 3049–3055.
- [34] Z.S. Yang, Y.L. Wang, G.C. Zhao, The interaction of copper-bipyridyl complex with DNA and cleavage to DNA, *Analytical Sciences: the International Journal of the Japan Society for Analytical Chemistry* 20 (2004) 1127–1130.
- [35] N. Shahabadi, M. Falsafi, N.H. Moghadam, DNA interaction studies of a novel Cu(II) complex as an intercalator containing curcumin and batho-phenanthroline ligands, *Journal of Photochemistry and Photobiology. B, Biology* 122B (2013) 45–51.
- [36] J. Liu, H. Zhang, C. Chen, H. Deng, T. Lu, L. Li, Interaction of macrocyclic copper(II) complexes with calf thymus DNA: effects of the side chains of the ligands on the DNA-binding behaviors, *Dalton Transactions: An International Journal of Inorganic Chemistry* (2003) 114–119.
- [37] N. Arshad, U. Yunus, S. Razzque, M. Khan, S. Saleem, B. Mirza, N. Rashid, Electrochemical and spectroscopic investigations of isoniazide and its analogs with dsDNA at physiological pH: evaluation of biological activities, *European Journal of Medicinal Chemistry* 47 (2012) 452–461.
- [38] S. Adsule, V. Barve, Di Chen, F. Ahmed, Q.P. Dou, S. Padhye, F.H. Sarkar, Novel Schiff base copper complexes of quinoline-2 carboxaldehyde as proteasome inhibitors in human prostate cancer cells, *Journal of Medicinal Chemistry* 49 (2006) 7242–7246.
- [39] A.W. Wallace, W.R. Murphy, J.D. Petersen, Electrochemical and photophysical properties of mono- and bimetallic ruthenium(II) complexes, *Inorganica Chimica Acta* 166 (1989) 47–54.
- [40] L.-Z. Li, C. Zhao, T. Xu, H.-W. Ji, Y.-H. Yu, G.-O. Guo, H. Chao, Synthesis, crystal structure and nuclease activity of a Schiff base copper(II) complex, *Journal of Inorganic Biochemistry* 99 (2005) 1076–1082.
- [41] R. Ramesh, S. Maheswaran, Synthesis, spectra, dioxygen affinity and antifungal activity of Ru(III) Schiff base complexes, *Journal of Inorganic Biochemistry* 96 (2003) 457–462.
- [42] Y. Anjaneyulu, R.P. Rao, Preparation, characterization and antimicrobial activity studies on some ternary complexes of Cu(II) with acetylacetone and various salicylic acids, *Synthesis and Reactivity in Inorganic and Metal-Organic Chemistry* 16 (1986) 257–272.
- [43] N.N. Al-Mohammed, Y. Alias, Z. Abdullah, R.M. Shakir, E.M. Taha, A.A. Hamid, Synthesis and antibacterial evaluation of some novel imidazole and benzimidazole sulfonamides, *Molecules: a Journal of Synthetic Chemistry and Natural Product chemistry. [Molecules (Basel, Switzerland)]* 18 (2013) 11978–11995.
- [44] A.Z. El-Sonbaty, M.A. Diab, A.A. El-Bindary, S.G. Nozha, Structural and characterization of novel copper(II) azodye complexes, *Spectrochimica Acta. Part A, Molecular and Biomolecular Spectroscopy* 83 (2011) 490–498.
- [45] A.S. Munde, A.N. Jagdale, S.M. Jadhav, T.K. Chondhekar, Synthesis and characterization of some transition metal complexes of unsymmetrical tetradentate schiff base ligand, *Journal of the Korean Chemical Society* 53 (2009) 407–410.
- [46] L. Li, K. Du, Y. Wang, H. Jia, X. Hou, H. Chao, L. Ji, Self-activating nuclease and anticancer activities of copper(II) complexes with aryl-modified 2,6-di(thiazol-2-yl)pyridine, *Dalton Transactions: An International Journal of Inorganic Chemistry* 42 (2013) 11576–11588.
- [47] (a) J. Tan, B. Wang, L. Zhu, *Journal of Biological Inorganic Chemistry: JBIC: a Publication of the Society of Biological Inorganic Chemistry* 14 (2009) 727–739; (b) V. Rajendiran, R. Karthik, M. Palaniandavar, H. Stoeckli-Evans, V.S. Perisami, M.A. Akbarsha, B.S. Srinag, H. Krishnamurthy, Mixed-ligand copper(II)-phenolate complexes: effect of coligand on enhanced DNA and protein binding, DNA cleavage, and anticancer activity, *Inorganic Chemistry* 46 (2007) 8208–8221; (c) X. Sheng, X. Guo, X.-M. Lu, G.Y. Lu, Y. Shao, F. Liu, Q. Xu, DNA binding, cleavage, and cytotoxic activity of the preorganized dinuclear zinc(II) complex of triazacyclononane derivatives, *Bioconjugate Chemistry* 19 (2008) 490–498.
- [48] M. Pitie, G. Prativiel, Activation of DNA carbon–hydrogen bonds by metal complexes, *Chemical Reviews* 110 (2010) 1018–1059.
- [49] D. Lahiri, T. Bhowmick, B. Pathak, O. Shameema, A.K. Patra, S. Ramakumar, A.R. Chakravarty, Anaerobic photocleavage of DNA in red light by dicopper(II) complexes of 3,3-dithiodipropionic acid, *Inorganic Chemistry* 48 (2009) 339–349.
- [50] J.A. Cowan, *Chemical nucleases*, *Current Opinion in Chemical Biology* 5 (2001) 634–642.
- [51] Y. Jin, J.A. Cowan, DNA cleavage by copper-ATCUN complexes. Factors influencing cleavage mechanism and linearization of dsDNA, *Journal of the American Chemical Society* 127 (2005) 8408–8415.
- [52] S. Mahapatra, J.A. Halfen, E.C. Wilkinson, L. Que Jr., W.B. Tolman, Modeling copper-dioxygen reactivity in proteins: aliphatic C–H bond activation by a new dicopper(II)-peroxo complex, *Journal of the American Chemical Society* 116 (1994) 9785–9786.
- [53] A. Chakraborty, P. Kumar, K. Ghosh, P. Roy, Evaluation of a Schiff base copper complex compound as potent anticancer molecule with multiple targets of action, *European Journal of Pharmacology* 647 (2010) 1–2.
- [54] S.K. Tomlinson, S.A. Melin, V. Higgs, D.R. White, P. Savage, D. Case, A.W. Blockstock, Schedule selective biochemical modulation of 5-fluorouracil in advanced colorectal cancer – a phase II study, *BMC Cancer* 2 (1990) 9.
- [55] J. Marmur, A procedure for the isolation of deoxyribonucleic acid from microorganisms, *Journal of Molecular Biology* 3 (1961) 208–218.
- [56] L.F. Tan, X.H. Liu, H. Chao, L.N. Ji, Synthesis, DNA-binding and photocleavage studies of ruthenium(II) complex with 2-(3'-phenoxyphenyl)imidazo[4,5-f][1,10]phenanthroline, *Journal of Inorganic Biochemistry* 101 (2007) 56–63.

- [57] J.B. Charies, N. Dattagupta, D.M. Crothers, Studies on interaction of anthracycline antibiotics and deoxyribonucleic acid: equilibrium binding studies on interaction of daunomycin with deoxyribonucleic acid, *Biochemistry* 21 (1982) 3933–3937.
- [58] S. Satyanarayanan, J.C. Davorusak, J.B. Charies, Tris(phenanthroline)ruthenium(II) enantiomer interactions with DNA: mode and specificity of binding, *Biochemistry* 32 (1983) 2573–2584.
- [59] M. Sonmez, M. Celebi, I. Berber, Synthesis, spectroscopic and biological studies on the new symmetric Schiff base derived from 2,6-diformyl-4-methylphenol with N-aminopyrimidine, *European Journal of Medicinal Chemistry* 45 (2010) 1935–1940.
- [60] R. Senthil Kumar, S. Arunachalam, DNA binding and antimicrobial studies of some polyethyleneimine-copper(II) complex samples containing 1,10-phenanthroline and l-theronine as co-ligands, *Polyhedron* 26 (2007) 3255–3262.
- [61] B.G. Tweedy, Possible mechanism for reduction of elemental sulfur by *monilinia fructicola*, *Phytopathology* 55 (1964) 910–914.
- [62] B.D. Clarkson, J.H. Burchenal, Preliminary screening of antineoplastic drugs, *Progress in Clinical Cancer* 1 (1965) 625–629.
- [63] F.F. D. Amour, F.R. Blood, D.A. Belden, *The Manual for Laboratory Work in Mammalian Physiology*. The University of Chicago Press, Chicago (1965) 23–24.
- [64] O.H. Lowry, N.T. Rosenbrough, A.L. Farr, R.J. Randall, Protein measurement with the folin phenol reagent, *The Journal of Biological Chemistry* 193 (1951) 265–275.
- [65] J.V. Dacie, *Practical Hematology*, second ed., J&A Churchill Ltd., London (, 1958, pp. 38–42.
- [66] K.R. Sheeja, G. Kuttan, R. Kuttan, Cytotoxic and antitumor activity of Berberine, *Amala Research Bulletin* 17 (1997) 73–76.